

# The velocity dispersion and mass profile of the Milky Way

Walter Dehnen<sup>\*</sup>, Dean E. McLaughlin, and Jalpesh Sachania

*Department of Physics & Astronomy, University of Leicester, Leicester, LE1 7RH*

Accepted 2006 March 30. Received 2006 February 17; in original form 2006 January 24

## ABSTRACT

We re-analyse the velocity-dispersion profile  $\sigma(r)$  at radii  $r > 10$  kpc in the Galactic stellar halo, recently derived by Battaglia et al. (2005), who concluded that, for a constant velocity anisotropy of the tracers, these data rule out a flat circular-speed curve for the Milky Way. However, we demonstrate that if one makes the natural assumption that the tracer density is truncated at  $r_t \gtrsim 160$  kpc and falls off significantly more steeply than  $r^{-3.5}$  at  $r \gtrsim 80$  kpc, then these data are consistent with a flat circular-speed curve and a constant velocity anisotropy comparable to that observed for halo stars in the Solar neighbourhood. We also consider a more detailed mass model with an exponential stellar disc and an extended non-isothermal dark-matter halo. In this two-component model, the Milky Way's virial radius and mass are  $r_{\text{vir}} \simeq 200$  kpc and  $M_{\text{vir}} \simeq 1.5 \times 10^{12} M_{\odot}$ . Still assuming the tracers' velocity anisotropy to be constant (at  $\beta \simeq 0.5$ ) we again find good agreement with the observed  $\sigma(r)$ , so long as the tracer density is truncated near the virial radius. These data by themselves do not allow to differentiate between different dark-halo or total-mass models for the Milky Way, nor between different velocity-anisotropy profiles for the tracers.

**Key words:** stellar dynamics – Galaxy: halo – galaxies: haloes – galaxies: structure

## 1 INTRODUCTION

The case for dark-matter haloes around spiral galaxies is predominantly based on the flatness of the rotation curves observed for gas out to large radii. For large elliptical galaxies at the centres of clusters, similarly strong evidence comes from X-ray haloes and from the kinematics of stellar tracers such as globular clusters out to a few effective radii (e.g., Côté et al. 2001, 2003; Richtler et al. 2004). For more isolated, ‘field’ ellipticals, however—or even those off-centre within clusters—the picture is somewhat less clear. For example, the projected velocity-dispersion profiles,  $\sigma(r)$ , of planetary nebulae in four such galaxies have been measured to several effective radii by Méndez et al. (2001) and Romanowsky et al. (2003). Although these data probe regions that are expected to be dynamically dominated by dark matter, the dispersion profiles are found to decrease outwards in a manner consistent with the assumption that light traces mass, i.e., that there are no extended dark haloes. However, unlike rotation curves,  $\sigma(r)$  profiles do not directly measure the total mass distribution, but are also affected by the density and velocity-anisotropy profiles of the tracers themselves. The importance of velocity anisotropy particularly has been emphasised by Mamon & Łokas (2005) and Dekel et al. (2005), who showed that falling dispersion profiles for elliptical galaxies are perfectly consistent with massive dark-matter haloes, in contrast to the original conclusion by Romanowsky et al. (2003).

Battaglia et al. (2005) have recently derived a velocity-dispersion profile for tracers at large radii in the Galactic stellar

halo (globular clusters, horizontal-branch and red-giant stars, and dSph satellites), finding a falling  $\sigma(r)$  much like in the isolated ellipticals. In analysing these data, they carefully consider the effects of velocity anisotropy and conclude that (1) a strictly flat circular-speed curve, corresponding to an isothermal *total* mass profile for our Galaxy, can be ruled out if the tracers' velocity anisotropy is spatially constant, and (2) a massive dark halo is consistent with the data only if its density falls off rapidly beyond  $r \gtrsim 100$  kpc and/or the stellar tracers are on predominantly near-circular orbits at these radii.

Underlying this argument by Battaglia et al. is an assumption that the stellar tracers follow a power-law density profile,  $\rho(r) \propto r^{-3.5}$  all the way out. In their Appendix B, these authors briefly addressed some possible consequences of relaxing this assumption, if the tracer velocity-anisotropy profile is assigned one specific form. However, they did not pursue any detailed modelling with the tracer  $\rho(r)$  allowed to deviate from a pure power law. The purpose of this paper is to develop such models. We find that, since the velocity data from Battaglia et al. reach more than halfway to the virial radius of the Galaxy—probing regions where the stellar density is unconstrained observationally, and even approaching what might be viewed as a natural ‘edge’ to the stellar halo—our ignorance of the detailed density distribution of the far stellar halo is at least as important as uncertainties in the tracers' velocity anisotropy when attempting to use the observed  $\sigma(r)$  to infer anything about the mass profile of the Galaxy.

Before considering the Milky Way data specifically, let us first review the factors affecting the velocity dispersion of a tracer population. We assume dynamical equilibrium and spherical symmetry,

<sup>\*</sup> Email: walter.dehnen@astro.le.ac.uk

denote the tracers' density profile by  $\rho(r)$ , and characterise the total galactic mass distribution by its circular-speed curve  $V_c^2(r) = GM_{\text{tot}}(r)/r$ . Then the radial component  $\sigma_r(r)$  of the tracer population's velocity dispersion must satisfy the Jeans equation

$$\frac{d}{dr}(\rho\sigma_r^2) + \frac{2\beta}{r}\rho\sigma_r^2 = -\rho\frac{V_c^2}{r}, \quad (1)$$

where  $\beta(r) = 1 - \sigma_\theta^2/\sigma_r^2$  is the usual velocity anisotropy parameter of the tracers ( $\beta = 0$  for isotropy,  $0 < \beta \leq 1$  for radial anisotropy, and  $\beta < 0$  for a tangentially biased velocity distribution).

In the simple situation of constant anisotropy  $\beta$ , and power laws for both the tracer density profile and the galaxy's circular-speed curve,  $\rho \propto r^{-\gamma}$  and  $V_c \propto r^\alpha$ , the Jeans equation requires that

$$\sigma_r^2 = \frac{1}{\gamma - 2\beta - 2\alpha} V_c^2(r) \quad \text{and} \quad \sigma_\theta^2 = \frac{1 - \beta}{\gamma - 2\beta - 2\alpha} V_c^2(r), \quad (2)$$

which reduces to equation (B2) of Battaglia et al. (2005) in the special case  $\alpha = 0$  ( $V_c = \text{constant}$ ). Thus, both components of  $\sigma$  are proportional to  $V_c$ , and they fall with radius if and only if the circular speed does. More realistically however,  $\beta$  and/or  $\gamma \equiv -d \ln \rho / d \ln r$  will be functions of radius; but we expect that at relatively large radii these will vary slowly enough for equation (2) to be still approximately valid and provide some heuristic insight into the general behaviour of  $\sigma(r)$ .

First, then, let  $\beta(r)$  decrease with radius, so that the tracer velocity distribution becomes more tangentially biased at larger radii. In this case, the denominators in equation (2) increase, so that  $\sigma_r(r)$  falls relative to  $V_c(r)$ . Thus Battaglia et al. (2005), working with strictly constant  $\gamma$ , conclude that a rather strongly decreasing anisotropy profile is necessary to reconcile their observed falling  $\sigma_r(r)$  profile with a standard Navarro, Frenk & White (1996, 'NFW') model for the mass distribution of the Milky Way.

For  $\gamma \gtrsim 2(1 + \alpha)$  (which holds in the Galactic halo and the outskirts of ellipticals), the effect on  $\sigma_\theta$  is dominated by the *numerator* in equation (2), such that a decreasing  $\beta(r)$  results in  $\sigma_\theta(r)$  rising relative to  $V_c(r)$ . The effect on the projected line-of-sight velocity dispersion is dominated by  $\sigma_\theta$  (but complicated by the projection) and results in the well-known degeneracy between the velocity anisotropy and the mass profile, which has plagued the interpretation of the velocity-dispersion profiles of ellipticals (for a recent exploration of this problem, see Mamon & Łokas 2005).

Second, suppose instead that  $\gamma(r)$  increases with radius (corresponding to  $\rho(r)$  decaying faster than a power law) while  $\beta$  remains constant. In this case, equation (2) tells us that both  $\sigma_r(r)$  and  $\sigma_\theta(r)$  fall relative to  $V_c(r)$ . In fact, if—for example—the tracer density decays exponentially, the anisotropy is fixed at  $\beta = 1/2$ , and the galaxy circular speed is constant ( $\alpha = 0$ ), then we find from an *exact* solution of the Jeans equation (1) that  $\sigma_r \propto r^{-1/2}$ : the velocity dispersion declines like that for a power-law  $\rho(r)$  in a Keplerian potential, even though the rotation curve is flat!

An even more drastic behaviour results from a tracer population which is truncated at a finite radius  $r_t$ . In this case,  $\gamma \rightarrow \infty$  as  $r \rightarrow r_t$  and from equation (2) we expect both components of the velocity dispersion to vanish in this limit. Thus, the falling  $\sigma_r(r)$  observed for the stellar halo of the Milky Way may still be consistent with a roughly flat circular-speed curve, if the tracer population effectively dies out at some large radius. This is the possibility that we pursue in more detail in Section 2. Note that for elliptical galaxies the tracer density is known, so that this problem does not arise in the interpretation of their velocity dispersions.

## 2 MODELLING THE MILKY WAY

### 2.1 A geometrical correction factor

The data collected by Battaglia et al. (2005) comprise heliocentric radial velocities corrected for the Solar motion relative to the Galactic centre, yielding velocities,  $v_{\text{GSR}}$ , in a Galactic standard of rest. However, these velocities must still be referred to the Galactic centre before comparing to any model. Thus, using spherical polar coordinates with the centre of the Milky Way at the origin, and the Sun on the  $z$ -axis at distance  $R_0 = 8$  kpc, we express the instantaneous distance  $d$  from an object to the Sun as

$$d^2 = r^2 + R_0^2 - 2rR_0 \cos \theta. \quad (3)$$

The time derivative of this is  $\dot{d} = v_{\text{GSR}} = a_r v_r + a_\theta v_\theta$ , where

$$a_r = (r - R_0 \cos \theta)/d \quad \text{and} \quad a_\theta = (R_0 \sin \theta)/d. \quad (4)$$

The velocity dispersion at a given Galactocentric radius  $r$  is estimated as the rms velocity averaged over all solid angles:

$$\sigma_{\text{GSR}}^2 = \langle a_r^2 \rangle \sigma_r^2 + \langle a_\theta^2 \rangle \sigma_\theta^2, \quad (5)$$

where  $\langle \cdot \rangle$  denotes the averaging over the sphere. Using  $a_r^2 + a_\theta^2 = 1$  and  $\sigma_\theta^2 = (1 - \beta)\sigma_r^2$ , we thus obtain

$$\sigma_{\text{GSR}}(r) = \sigma_r \sqrt{1 - \beta(r) A(r)} \quad (6)$$

with  $A(r) \equiv \langle a_\theta^2 \rangle$  a monotonically declining function of radius:

$$A(r) = \frac{r^2 + R_0^2}{4r^2} - \frac{(r^2 - R_0^2)^2}{8r^3 R_0} \ln \left| \frac{r + R_0}{r - R_0} \right|. \quad (7)$$

The correction factor in equation (6) becomes unity for an isotropic velocity distribution ( $\beta = 0$ ), since in this case the velocity dispersion is independent of direction. For non-zero  $\beta$ , the correction is greatest for small  $r$ , where  $A(r)$  becomes largest ( $A = 1/2$  at  $r = R_0$  and  $A = 2/3$  at  $r = 0$ ), while for  $r \gg R_0$ ,  $A \ll 1$  and  $\sigma_{\text{GSR}} \approx \sigma_r$ .

Unfortunately, Battaglia et al. (2005) use an incorrect formula to convert between  $\sigma_r$  and  $\sigma_{\text{GSR}}$  [their equation (3) corresponds to (6) above], which gives a correction factor larger than unity for  $\beta = 0$ . This significantly affects the predicted  $\sigma_{\text{GSR}}$  only at radii  $r \lesssim 30$  kpc. However, this is where the uncertainties in the observed  $\sigma_{\text{GSR}}$  are smallest, resulting in substantially erroneous  $\chi^2$  for any model fits.

### 2.2 Simple models with truncated tracer populations

Let us now employ some simple, fully analytic models of truncated density profiles to demonstrate that the Milky Way  $\sigma_{\text{GSR}}$  data are consistent with a flat circular-speed curve, i.e., an isothermal total-mass distribution. We assume that the density of the tracer population, outside of some (small) core radius, is given by

$$\rho(r) \propto \begin{cases} (r^{-\gamma/n} - r_t^{-\gamma/n})^n & \text{for } r < r_t, \\ 0 & \text{for } r \geq r_t, \end{cases} \quad (8)$$

which is plotted in Fig. 1 for  $\gamma = 3.5$  and  $n = 1, 2$ , or  $3$ . At small radii, say  $r \lesssim 0.5r_t$ , the profiles in this graph are hardly distinguishable from a pure power-law  $\rho \propto r^{-3.5}$ , which matches the density of the Galactic stellar halo out to  $r \sim 50$  kpc (Morrison et al. 2000; Yanny et al. 2000). The abruptness of the truncation towards larger radii depends on the parameter  $n$ . We have used the online database of Harris (1996) to verify that, for  $r_t \gtrsim 150$  kpc, a model with  $\gamma = 3.5$  and  $n = 2$  provides a good description of the density of Galactic globular clusters at  $r \gtrsim 3$  kpc. This is thus the model we use for all applications to data in this paper.

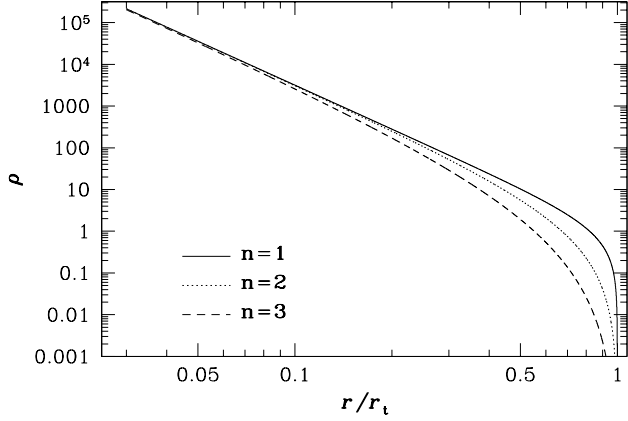


**Figure 1.** Truncated density profiles of equation (8) with  $\gamma = 3.5$  and  $n = 1$  (solid),  $n = 2$  (dotted), or  $n = 3$  (dashed).

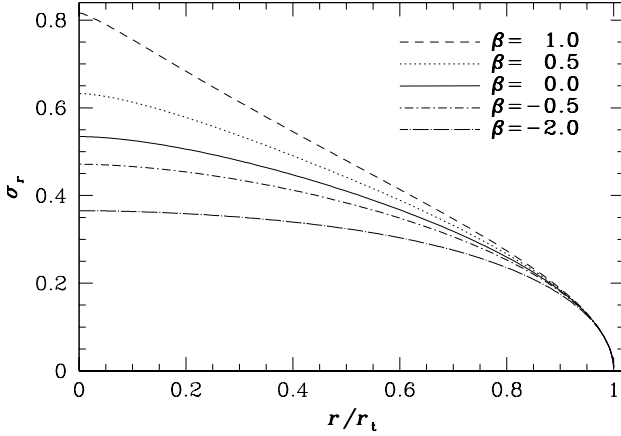


**Figure 2.** Radial velocity-dispersion profile for a tracer population with constant anisotropy  $\beta$  and truncated density (8) with  $\gamma = 3.5$  and  $n = 2$ , embedded in a gravitational potential with constant circular speed ( $\alpha = 0$ ). For a slightly falling circular-speed curve, such as predicted for dark-matter haloes,  $\sigma_r$  falls off slightly faster.

Given equation (8), a constant anisotropy  $\beta$  for the tracers, and a power-law circular-speed curve,  $V_c(r) = V_0(r/r_t)^\alpha$ , the radial component of the velocity dispersion can be obtained analytically from the Jeans equation (1) for integer  $n$ :

$$\sigma_r^2 = \frac{V_0^2}{(x^{-\gamma/n} - 1)^n x^{2\beta}} \sum_{k=0}^n \binom{n}{k} (-1)^{n-k} h\left(\frac{\gamma k}{n} - 2\alpha - 2\beta; x\right) \quad (9)$$

with  $x \equiv r/r_t$  and

$$h(q; x) \equiv \int_x^1 \frac{du}{u^{q+1}} = \begin{cases} -\ln x & \text{for } q = 0, \\ \frac{1}{q}(x^{-q} - 1) & \text{for } q \neq 0. \end{cases} \quad (10)$$

In the limit  $r \rightarrow r_t$ ,  $\sigma_r \rightarrow 0$ , as the simple considerations of Section 1 already implied it must. (In this limit equation (9) is numerically unstable against truncation errors, but instead one may use

$$\frac{\sigma_r^2(r)}{V_c^2(r)} = \frac{\epsilon}{n+1} \left[ 1 + \left( n + 1 + 2(\alpha + \beta) - \frac{\gamma + n}{2} \right) \frac{\epsilon}{n+2} + O(\epsilon^2) \right] \quad (11)$$

with  $\epsilon = 1 - x > 0$ .)

In Fig. 2, we plot  $\sigma_r(r)$  for a flat rotation curve ( $\alpha = 0$ ) and  $\gamma = 3.5$ ,  $n = 2$  (appropriate to the situation in the Milky Way stel-

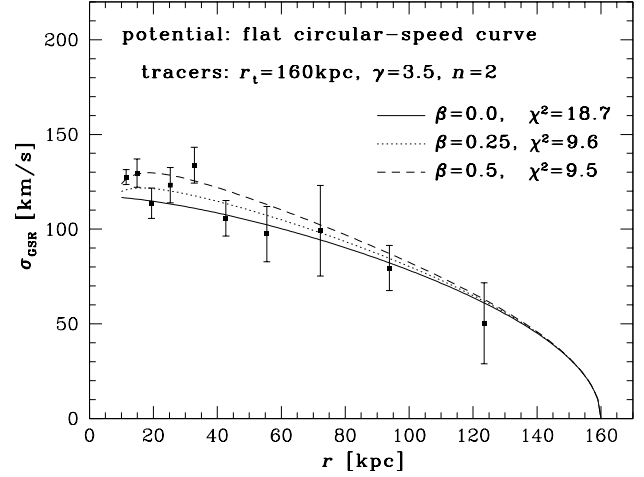


**Figure 3.** Comparison of truncated power-law models embedded in a flat circular-speed curve of  $V_c = 220 \text{ km s}^{-1}$  to the Battaglia et al. (2005) data for the Milky Way. Slightly better fits could be achieved with smaller truncation radius  $r_t$  or a slightly falling circular-speed curve.

lar halo), and for various  $\beta$ . Evidently, the velocity dispersion declines over much the whole range of radii, even though the density deviates from the power-law form only for large radii. The physical reason is that in order to achieve a truncation in density, orbits that reach near  $r_t$  must be de-populated relative to a non-truncated model. These orbits, however, would have contributed at smaller radii with rather large  $v_r$ . Note that all the models presented in Fig. 2 are physical in the sense that they possess a non-negative distribution function of the form  $f(E, L) = L^{-2\beta} g(E)$ .

In Fig. 3, we compare these simple models (after applying the geometric correction of Section 2.1) to the  $\sigma_{\text{GSR}}(r)$  data of Battaglia et al. (2005). The tracer density again has  $\gamma = 3.5$  and  $n = 2$ , and we set the truncation radius to  $r_t = 160 \text{ kpc}$ . We assume a constant circular speed of  $V_c = 220 \text{ km s}^{-1}$  and constant  $\beta$  of 0 (isotropic), 0.25, or 0.5 (radially anisotropic). All these models correctly reproduce the decline of  $\sigma$  towards larger radii.

At small radii ( $r \lesssim 40 \text{ kpc}$ ), the isotropic model (solid curve) cannot account for the observed dispersion, but falls significantly below. Since at these radii  $\gamma \approx 3.5$  is observationally secure, we have from equation (2) that  $\sigma_r \approx V_c / \sqrt{3.5} = 0.53 V_c$  for any isotropic model if  $V_c(r)$  is near-flat just outside the solar circle. A possible explanation of the observed high  $\sigma_{\text{GSR}}$  for a tracer population with isotropic velocities requires a circular-speed curve which rises like  $V_c \propto r^{0.1}$  out to  $r \sim 30 \text{ kpc}$  (where then  $V_c = 250 \text{ km s}^{-1}$ ). Alternatively and more reasonably, the data are consistent with a near constant  $V_c = 220 \text{ km s}^{-1}$  if the tracer velocities at  $r \lesssim 40 \text{ kpc}$  are slightly radially biased with  $\beta = 0.25 - 0.5$ , comparable to what has been derived for halo stars in the Solar neighbourhood (Chiba & Yoshii 1998; Gould 2004).

### 2.3 More sophisticated models

The above analysis shows that the Battaglia et al. (2005) data are in fact consistent with constant velocity anisotropy for the tracers and an isothermal total mass distribution for the Milky Way. We can further ask whether the same data are consistent with a more detailed model explicitly including both a stellar disc—which is well known to dominate the total mass inside the Solar circle (e.g., Dehnen & Binney 1998), and still contributes  $\gtrsim 10\%$  to the mass

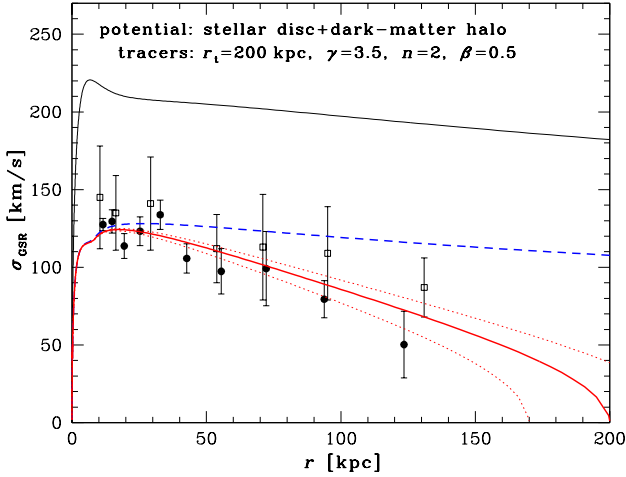


**Figure 4.** Two-component mass model for the Milky Way, and the velocity-dispersion profile for a tracer population in the stellar halo. The thin, solid (black) curve is the total circular-speed curve  $V_c(r)$  of the model (see eqs. [12] and [13]). The bold, solid (red) curve running through the data is the predicted GSR velocity-dispersion profile for a tracer population with a density profile truncated at  $r_t = 200$  kpc (see text for details) and with a spatially constant velocity anisotropy  $\beta = 0.5$ . The thinner, dotted (red) curves bracketing this are the predicted  $\sigma_{\text{GSR}}$  for  $\beta = 0.5$  still, but with truncation radii  $r_t = 170$  kpc and  $r_t = 230$  kpc. The bold, dashed (blue) curve above these is the  $\sigma_{\text{GSR}}$  that would obtain with  $\beta = 0.5$  and  $\rho(r) \propto r^{-3.5}$  at all radii (no truncation). Data points are from Battaglia et al. (2005) (filled circles) and from Harris (2001) (open squares).

at 50 kpc—and an extended dark-matter halo which is (as per cosmological  $N$ -body simulations) non-isothermal.

We first specify an exponential stellar disc with rotation curve

$$V_{c,d}^2(r) = \frac{GM_d(r)}{r} = \frac{GM_{d,\text{tot}}}{r} \left[ 1 - \left( 1 + \frac{r}{r_d} \right) \exp\left(-\frac{r}{r_d}\right) \right], \quad (12)$$

where  $M_{d,\text{tot}} = 5.8 \times 10^{10} M_\odot$  and  $r_d = 2.4$  kpc according to Dehnen & Binney (1998).

Second, we take a dark-matter halo from the family of models developed by Dehnen & McLaughlin (2005). Specifically, we assume that the halo follows the scaling  $\rho_h/\sigma_{r,h}^3 \propto r^{-35/18}$  (consistent with simulations) and has an isotropic velocity distribution at its centre (but may be anisotropic elsewhere). Such a halo has a density cusp  $\rho_h \rightarrow r^{-7/9}$  in the limit  $r \rightarrow 0$ , and  $\rho_h \rightarrow r^{-31/9}$  as  $r \rightarrow \infty$ . Thus, it has a finite total mass, and its circular-speed curve is

$$V_{c,h}^2(r) = \frac{GM_h(r)}{r} = \frac{GM_{h,\text{tot}}}{r} \left[ \frac{r^{4/9}}{r^{4/9} + r_0^{4/9}} \right]^5, \quad (13)$$

from equation (20f) of Dehnen & McLaughlin (2005).

To fix the halo parameters, we specify the value of the *total* circular speed,  $V_c^2 = V_{c,d}^2 + V_{c,h}^2$ , at two Galactocentric radii: at the position of the Sun,  $r = 8$  kpc, we require  $V_c = 220$  km s $^{-1}$ , while at  $r = 50$  kpc we adopt  $V_c = 205$  km s $^{-1}$ . This latter value corresponds to a total mass of  $M_d + M_h = 4.9 \times 10^{11} M_\odot$  inside  $r = 50$  kpc, chosen in order to agree with the analysis of Kochanek (1996, see also Rohlfs & Kreitschmann 1988). These two constraints then imply  $M_{h,\text{tot}} = 1.10 \times 10^{13} M_\odot$  and  $r_0 = 40.5$  kpc.

The total mass  $M_{h,\text{tot}}$  here is obtained formally by integrating the dark-matter density profile to infinity, but physically more meaningful is the halo mass within finite radii corresponding to specific over-densities relative to the critical  $\rho_c = 3H_0^2/8\pi G$ .

First, in a ‘concordance’  $\Lambda$ -CDM cosmology with  $\Omega_m = 0.3$  and  $\Omega_\Lambda = 0.7$ , the virial radius of a halo is that within which the average density  $3M_h(r_{\text{vir}})/4\pi r_{\text{vir}}^3$  is equal to  $337\rho_c$  (e.g., Bullock et al. 2001). With  $H_0 = 70$  km s $^{-1}$  Mpc $^{-1}$ ,  $r_{\text{vir}} \approx 200$  kpc and  $M_{\text{vir}} \approx 1.5 \times 10^{12} M_\odot$  for our model, both of which are reasonable for an  $L_*$  galaxy like the Milky Way. Alternatively, haloes are commonly measured by the radius  $r_{200}$  within which the average density is  $200\rho_c$ . In our case,  $r_{200} \approx 250$  kpc and  $M_{200} \approx 1.75 \times 10^{12} M_\odot$ . For comparison with numbers given by Battaglia et al. (2005), the total mass inside 120 kpc is  $M(r \leq 120 \text{ kpc}) = 1.05 \times 10^{12} M_\odot$ .

A scale of interest in connection with numerical simulations of dark-matter haloes is the radius  $r_{-2}$  at which the local logarithmic slope of the density profile is  $d \ln \rho_h / d \ln r = -2$ . In our model,  $r_{-2} = (11/13)^{9/4} r_0 = 27.8$  kpc, and the ratio  $r_{200}/r_{-2} = 9$  is nicely consistent with the values found by Navarro et al. (2004) for simulated haloes with masses in the range  $M_{200} = 1 - 2 \times 10^{12} h^{-1} M_\odot$ .

To predict the kinematics of tracers in the stellar halo, we use the density model for the tracers that has already been employed in section 2.2, i.e., equation (8) with  $\gamma = 3.5$  and  $n = 2$ , although we set the truncation radius  $r_t = r_{\text{vir}} = 200$  kpc, somewhat larger than the value used in Figure 3. We then solve the Jeans equation (1) for an assumed spatially constant velocity anisotropy  $\beta$ , and apply the geometric correction in equation (6). This yields a model  $\sigma_{\text{GSR}}(r)$ , which is compared to the Battaglia et al. (2005) data to compute  $\chi^2$ . The minimum  $\chi^2 = 9.5$  (for 10 data points) is achieved with  $\beta = 0.5$ . As was mentioned above, this slight radial bias is consistent with observations of halo stars in the Solar neighbourhood (Chiba & Yoshii 1998; Gould 2004).

Figure 4 shows our best-fit  $\sigma_{\text{GSR}}$  profile against the Battaglia et al. data, plus another estimate of the stellar-halo velocity-dispersion profile from Harris (2001). The latter is also constructed from velocity data for globular clusters, RR Lyrae stars, and dwarf spheroidals, and so is not independent of the Battaglia et al. profile; thus, we have not used it in determining  $\chi^2$  for our models. However, this alternate profile serves to confirm the overall sense of the Battaglia et al. results (and to emphasise their uncertainty at the largest radii). We have also plotted in Figure 4 alternate models in which the tracers still have constant  $\beta = 0.5$  but are truncated at  $r_t = 170$  or  $230$  kpc. The bold, dashed curve which declines only gradually towards large radius is the velocity-dispersion profile assuming the tracer density profile to be an untruncated pure power law  $\rho \propto r^{-3.5}$ . This is the assumption made by Battaglia et al. (2005) in their modelling, and it clearly has a dramatic—even dominant—influence on the anisotropy profiles they require in order to fit the observed  $\sigma_{\text{GSR}}(r)$ .

### 3 DISCUSSION

Comparing Figures 3 and 4, it is clear that in the latter we are able to describe the observed  $\sigma_{\text{GSR}}(r)$  profile with a larger assumed truncation radius for the stellar-halo tracers than in the former, and also that a constant  $\beta = 0.5$  predicts slightly lower velocity dispersions at small radii in our (disc+halo) mass model than in the constant- $V_c$  model. These points simply reflect that the total circular speed given by equations (12) and (13) decreases monotonically with radius for  $r > 6.6$  kpc (which adds to the effect of a truncated tracer density in driving the decline of  $\sigma_{\text{GSR}}$ ), and in fact is less than 220 km s $^{-1}$  at all radii covered by the Battaglia et al. (2005) or Harris (2001) data (so for fixed  $\gamma$ , a slightly higher  $\beta$  is required to give the same normalisation to the tracers’  $\sigma_r$ , as can be seen from eq. [2]).

Even so, all of the anisotropic models illustrated here fit the data equally well, and thus the tracer velocity-dispersion profile alone *cannot* be used to distinguish between different (reasonable) models for the total mass distribution in the Milky Way. Conversely, beyond concluding simply that the observed  $\sigma_{\text{GSR}}(r)$  profile is consistent with a tracer density profile that falls steeply at  $r \gtrsim 80$  kpc, we cannot use these kinematics to infer anything more detailed about the behaviour of  $\rho(r)$  for the far stellar halo.

Nor can strong constraints be placed on the velocity anisotropy of the tracer population. In the context of a spatially constant  $\beta$ , as we have assumed, all that can be said with any confidence is that a slight radial bias ( $\beta \sim 0.2 - 0.6$ , depending on the Galactic mass model) is required to explain the amplitude of  $\sigma_{\text{GSR}}$  at  $r \lesssim 40$  kpc. If the assumed form of the total mass distribution deviates significantly from the models with constant or slowly-varying  $V_c(r)$  that we have explored, then a variety of  $\beta(r)$  behaviour is likely allowed by the data.

Clearly, untangling the degeneracies between the total  $M(r)$  and tracer  $\rho(r)$  and  $\beta(r)$ , to put quantitative limits on any one profile from knowledge of the others, is a daunting task that will require much closer attention to a wider variety of data beyond just  $\sigma_{\text{GSR}}(r)$ . For example, the models for  $V_c(r)$  that we have worked with here are extremely simple and would surely require some modification in detail if we attempted to take accurately into account the many other constraints on the Galactic mass distribution. But more detailed modelling will also have to allow for the fact that the tracers contributing to the Battaglia et al. (2005) and Harris (2001) velocity-dispersion profiles are very much a ‘mixed bag’: the halo globular clusters, for instance, may not have the same anisotropy profile as the field RR Lyrae and red giants; and the satellite dwarf spheroidals likely do not follow the same density profile as the stars and globulars. Ideally, we need information on *separate*  $\sigma(r)$ ,  $\rho(r)$ , and  $\beta(r)$  profiles for each of the different tracer populations. Current data simply do not provide this.

## 4 SUMMARY

We have demonstrated in this study that the falling velocity dispersion found by Battaglia et al. (2005) in the outer stellar halo of the Milky Way is consistent with a constant (and reasonable) velocity anisotropy for the stellar tracers, and either a perfectly flat circular-speed curve (i.e. an isothermal total mass distribution) or a standard CDM dark-matter halo combined with an exponential stellar disc. By contrast, Battaglia et al. argued that their data were inconsistent with  $V_c$  and  $\beta$  both being strictly constant, and that they required a strongly varying (and rather unusual)  $\beta(r)$  profile to be made compatible with the common Navarro et al. (1996) model for a dark-matter halo.<sup>1</sup>

As we have emphasised, the primary reason for the difference between our conclusions and theirs is that we allow for the tracer density to die out at  $r \gtrsim 160$  kpc, close to the Milky Way’s virial radius, whereas Battaglia et al. assume that  $\rho \propto r^{-3.5}$ , which is valid for  $r \lesssim 50$  kpc, continues to hold for all larger radii. An incorrect transformation from modelled  $\sigma_r(r)$  to observed  $\sigma_{\text{GSR}}(r)$  on the part of Battaglia et al. (see Section 2.1) has certainly also contributed to

the discrepancy, insofar as it affected the  $\chi^2$  values of their detailed model fits.

As we discussed, these data by themselves are insufficient for differentiation between different total-mass models for the Galaxy, nor between different velocity-anisotropy profiles for the tracers. This is essentially because the measured  $\sigma(r)$  depends on both of the above (the well-known degeneracy between velocity anisotropy and mass profile) and on the tracer’s density profile, which is little constrained observationally at  $r \gtrsim 50$  kpc.

## ACKNOWLEDGEMENTS

We thank Giuseppina Battaglia for providing us with the Milky Way velocity-dispersion data points from her Figure 1, in electronic form. DEM is supported by a PPARC standard grant, and research in theoretical astrophysics at the University of Leicester is also supported by a PPARC rolling grant.

## REFERENCES

- Battaglia G., Helmi A., Morrison H., Harding P., Olszewski E. W., Mateo M., Freeman K. C., Norris J., Shtetman S. A., 2005, MNRAS, 364, 433
- Bullock J. S., Kolatt T. S., Sigad Y., Somerville R. S., Kravtsov A. V., Klypin A. A., Primack J. R., Dekel A., 2001, MNRAS, 321, 559
- Chiba M., Yoshii Y., 1998, AJ, 115, 168
- Côté P., McLaughlin D. E., Cohen J. G., Blakeslee J. P., 2003, ApJ, 591, 850
- Côté P., McLaughlin D. E., Hanes D. A., Bridges T. J., Geisler D., Merritt D., Hesser J. E., Harris G. L. H., Lee M. G., 2001, ApJ, 559, 828
- Dehnen W., Binney J. J., 1998, MNRAS, 294, 429
- Dehnen W., McLaughlin D. E., 2005, MNRAS, 363, 1057
- Dekel A., Stoehr F., Mamon G. A., Cox T. J., Novak G. S., Primack J. R., 2005, Nature, 437, 707
- Gould A., 2004, ApJ, 607, 653
- Harris W. E., 1996, AJ, 112, 1487
- Harris W. E., 2001, in Saas-Fee Advanced Course 28: Star Clusters Globular cluster systems. p. 223
- Kochanek C. S., 1996, ApJ, 457, 228
- Mamon G. A., Łokas E. L., 2005, MNRAS, 363, 705
- Méndez R. H., Riffeser A., Kudritzki R.-P., Matthias M., Freeman K. C., Arnaboldi M., Capaccioli M., Gerhard O. E., 2001, ApJ, 563, 135
- Morrison H. L., Mateo M., Olszewski E. W., Harding P., Dohm-Palmer R. C., Freeman K. C., Norris J. E., Morita M., 2000, AJ, 119, 2254
- Navarro J. F., Frenk C. S., White S. D. M., 1996, ApJ, 462, 563
- Navarro J. F., Hayashi E., Power C., Jenkins A. R., Frenk C. S., White S. D. M., Springel V., Stadel J., Quinn T. R., 2004, MNRAS, 349, 1039
- Richtler T., Dirsch B., Gebhardt K., Geisler D., Hilker M., Alonso M. V., Forte J. C., Grebel E. K., Infante L., Larsen S., Minniti D., Rejkuba M., 2004, AJ, 127, 2094
- Rohlf K., Kreitschmann J., 1988, A&A, 201, 51
- Romanowsky A. J., Douglas N. G., Arnaboldi M., Kuijken K., Merrifield M. R., Napolitano N. R., Capaccioli M., Freeman K. C., 2003, Science, 301, 1696
- Yanny B. et al., 2000, ApJ, 540, 825

<sup>1</sup> When Battaglia et al. (2005) discuss ‘NFW’ or ‘truncated flat’ or ‘isothermal’ haloes, they really model the *total* Galactic mass distribution with those functions. But as we discussed in connection with Figure 4, the stellar disc contributes significantly to the total circular speed out to tens of kpc, and the total  $V_c(r)$  differs from that of the dark halo until very large radii.